Spouting Behaviors of Binary Mixtures of Cylindroid and Spherical Particles

Xuejiao Liu, Wenqi Zhong, Xiaofeng Jiang, and Baosheng Jin
Key Laboratory of Energy Thermal Conversion and Control of Ministry of Education, School of Energy and Environment, Southeast University, Nanjing 210096, China

DOI 10.1002/aic.14636
Published online October 9, 2014 in Wiley Online Library (wileyonlinelibrary.com)

Spouting behaviors of cylindroid and spherical particles in a spouted bed are experimentally investigated. The characteristics of flow pattern and pressure drop of the binary mixtures are figured out and three kinds of cylindroid particles with different sizes and shapes are involved in experiments to discuss effects of particle size and shape on the spouting behaviors in beds. The emphasis is laid on the influence of the volume fraction of cylindroid particles, X_c, on the spouting phenomena, including the total pressure drop, the minimum spouting velocity, and fountain height. Results show that, the shapes and sizes of cylindroid particles, mainly including equivolume diameter and aspect ratio, significantly affect the spouting behaviors. There is a maximum volume fraction, $X_{c,max}$, for each kind of cylinders to maintain the stable fountain at a certain gas velocity. With the same gas velocity, $X_{c,max}$ is lower for the cylinders with higher aspect ratio. *AIChE J*, 61: 58–67, 2015
Keywords: particle mixing, cylindroid particles, spouted bed, gas–solid flow

Introduction

Biomass is considered as the most promising renewable energy source to contribute to the energy requirement in modern society, benefiting from its greenhouse gas neutral and the feasibility to reuse forestry and agricultural wastes.[1–3] A wide variety of efforts have been made worldwide to develop the biomass utilization technology, and three main thermal-chemical processes, that is, combustion, gasification, and pyrolysis, usually based on fluidization, show significantly excellent prospects to convert wood, energy crops, agricultural and forestry wastes to liquid, solid, and gaseous fuels.[2–5] Many typical fluidization process equipments, for example, fluidized beds, spouted beds, and spout-fluid beds have been used to handle the biomass particles in many attempts.[1,5–8] The spouted bed reactors are proved to be of great potential to treat biomass particles due to their ability to deal with particles with larger sizes or larger size distributions and to provide good particle circulation, effective fluid-particle contact, and high rates of heat and mass transfer.[9–11] Especially, the decouple residence times of gas and solids in spouted beds, which effectively reduce the gas residence time and unwanted secondary biomass reactions, increase the interest to use the spouted bed reactors to carry out catalytic pyrolysis of biomass.

In practice, biomass particles always are of special properties, and they are usually large in size, long and thin in shape, and low in density.[1] Direct spouting the nonstandard biomass particles in spouted beds is quite difficult, thus, inert material is often required in the reactors.[1,5,7,12] The inert particles, mixing with the biomass in beds, not only effectively improve the flow behaviors of biomass but also act as high-efficient heat transfer medium.[5,7] Compared with handling homogeneous spherical particles, the hydrodynamic characteristics of spouting a mixture of long and thin nonspherical biomass particles and fine spherical inert particles in spouted beds inevitably become more complicated. Understanding the spouting behaviors of the mixture is of fundamental importance to develop spouted bed reactor in biomass thermal-chemical processes.

Research on this aspect is very limited, and many essential issues are still unknown, for example, what spouting characteristics the mixture presents in the spouted bed? How the shape and size of biomass particles affect the spouting behaviors, and what size can achieve the satisfactory spouting state in the spouted bed? What is the optimal proportion of biomass particle that the unit can handle? Answers to these questions are of the essence to the application of spouted beds in biomass technology. However, the complicated properties of biomass particles bring too many coupled factors, for instance, particle shape, size, and texture, to affect the spouting and mixing results in spouted beds. Unraveling and figuring out influence rules of these factors is of great challenge and requires a huge effort. Relevant research is urgently required.

In this article, cylindroid bamboo particles are selected to characterize biomass and the glass beads are adopted as inert particles. The spouting and mixing mechanism of cylindroid particles and spherical particles in spouted bed were experimentally investigated. The characteristics of flow pattern and pressure drop of the binary mixture are figured out and three kinds of cylindroid particles with different sizes and shapes

Correspondence concerning this article should be addressed to W. Zhong at wqzhong@seu.edu.cn.

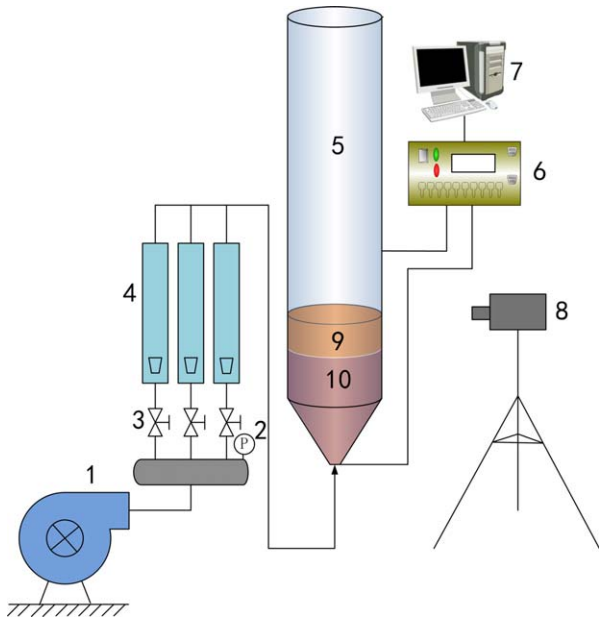

Figure 1. Schematic of diagram of experimental setup: (1) roots blower; (2) pressure gauge; (3) control valve; (4) rotameter; (5) spouted bed; (6) differential pressure sensor; (7) computer; (8) digital CCD; (9) Cylindroid particles; (10) glass beads.

[Color figure can be viewed in the online issue, which is available at wileyonlinelibrary.com.]

are involved in experiments to reveal the effects of particle size and shape on the spouting and mixing behaviors in beds. In addition, influence of the volume fraction of cylindroid particles on the spouting phenomena, including the total pressure drop, the minimum spouting velocity, fountain height, is emphatically discussed.

Experiments

The experimental apparatus used in this study includes a cone-based cylindrical Plexiglas column, a gas supply system, an imaging system, and a multichannel differential pressure signal sampling system, which has been well shown in our previous work.[13] Figure 1 gives the schematic diagram of the experimental setup. In Figure 1, the internal diameter of cylindrical column, D, is 200 mm and the height is 1500 mm. The included angle of the conical base is 60°, and the diameter of the gas inlet orifice, D_i, is 20 mm. The spouting gas supplied by a Roots blower is introduced into the column through the inlet orifice and the gas flow can be manually controlled by a valve and the flow rates are obtained by rotor flow meters. Two holes were drilled as the pressure measuring points on the side of column and the distances from the bed bottom are 0 and 640 mm, respectively. A multichannel differential pressure signal transmitter with a scale of 0–50 kPa is used to measure the pressure drops of bed and converts them into voltage signals which are finally sent to computer through an A/D converter.

The spouting and mixing processes are recorded with a high speed digital camera (Nikon Coolpix L200) which is setup in front of the spouted bed. A graduated paper tape is vertically pasted on the surface of column to indicate the heights of bed levels and fountains.

Closely sized spherical glass beads of mean diameter of 2.6 mm, density of 2600 kg/m^3 were used as inert particles in this study, for the reason that the glass bead is one of the most common particles used in the spouting experiments and its excellent spouting characteristics have been well known by researchers.[9] The spouting characteristics of three sizes of bamboo particles mixing with the inert particles were examined, respectively. The bamboo particles are cylinders and their detailed properties are shown in Table 1. In experiments, for each kind of bamboo particles, their volume fraction in mixture, X_c, is varied from 0 to 1.0, and the spouting behaviors of the mixtures with different volume ratios of bamboo particles and glass bead are investigated.

In each experiment, the total volume, V, inside the spouted bed under the specified static bed height were calculated first. The corresponding volume of bamboo particles was $V_c = X_c \times V$, while the volume of glass beads was $V_s = (1 - X_c) \times V$. At the beginning of the experiment, these two kinds of particles, respectively, were added into the spouted beds with the given volumes. The initial bed was loosely packed and completely layered: the bottom layer was glass bead, while the upper layer is bamboo particle, which specific distribution is one of the very likely starting states in the potential biomass thermal conversion processes.[7,14] And more importantly, this separated distribution is simpler and easier to control in each run, and starting from the extreme initial state, more typical operational parameters will be obtained, for example, the maximum pressure drop. In addition, taking the complete separation of the biomass and inert particles as the initial distribution can facilitate the more effective and convincing evaluation on the mix ability of spouted beds.

The ambient air was introduced through the gas inlet orifice with the gradually increasing flow rate, until stable external spouting is reached. During this flow ascending process, spouting information including pressure drops, flow patterns, and fountain heights, respectively, were recorded by the multichannel differential pressure signal sampling system and the imaging system. Next, the air flow rate was gradually decreased until it was close to zero. The inlet-based minimum spouting velocity, u_{ms}, or the superficial minimum spouting velocity, U, was captured at the point when stable external spouting collapses in the flow descending process. In current system, the relationship between inlet-based gas velocity and the superficial gas velocity is $U = u/(D/D_i)^2$, that is, $U = u/100$. Valuable information about pressure drops and flow patterns was also acquired.

Table 1. Properties of Particles

Particle		$d \times l$ (mm × mm)	d_v (mm)	ρ_p (kg/m^3)	φ	Asr (l/d)	ε_0
Glass bead			2.6	2600	1.00		0.37
Bamboo particles	Cylinder A	8 × 10	9.9	590	0.87	1.25	0.32
	Cylinder B	4 × 10	6.2	590	0.80	2.5	0.35
	Cylinder C	4 × 20	7.8	590	0.69	5	0.42

Results and Discussion

Evolution of the spouting process

For the binary mixture of bamboo particles of Cylinder A ($d \times l = 8 \times 10$ mm^2) and the glass beads as an example, the typical process of spouting the cylindroid and spherical particles and the evolution of total pressure drop are illustrated in Figure 2. The volume fraction of Cylinders A is $X_c = 0.4$ and the initial static bed height is $H_0 = 300$ mm. The total transitions of flow pattern and evolution of pressure drop are generally similar to that of spouting homogenous spherical particles, but the additional mixing and segregating behaviors bring some unique features.

The experiment starts with a loosely packed bed, in which two kinds of particles are completely segregated. The glass beads are in the bottom of the bed, while the Cylinder A particles are in the upper layer. When the gas is introduced into the column through the nozzle with low gas flow rate, only the glass beads near the nozzle starts to circulate, while the glass beads in upper bed level and the Cylinder A particles are still static. Further increase in gas flow rate expands the regime, where glass beads are in motion and more glass beads are involved in circulation. The internal spout is established and grows with the increasing gas velocity. At the same time, the bed surface moves upward visibly. During this period, the total pressure drop increases with the increasing gas velocity and reaches a peak value (point b) as $u = 39$ m/s ($U = 0.39$ m/s). This peak value is defined as the maximum pressure drop, Δp_{max}. Further increase in the gas velocity leads to the decreasing total pressure drop before the curve reaches the point c. This regime during which the internal spout expands within the layer of glass beads and the glass beads and cylindroid particles are completely segregated is labeled as the regime of complete segregation in Figure 2.

When the inlet gas velocity increases to $u = 58$ m/s ($U = 0.58$ m/s, point c in pressure drop curve), the internal spout just reaches the interface between glass beads and Cylinder A particles. The packed cylinder particles suddenly become more loosely, and the surface of the bed consequently rises. Initial local mixing behaviors occur from this moment.

When the gas flow rate continues to increase, the Cylinder A particles start to be involved in the internal spout and the mixture of Cylinder A particles and glass beads together move to the bottom of the bed and join in the circulation of internal spout. This process is corresponding to the regime from points c to d in the pressure drop curve. From the point c ($u = 58$ m/s or $U = 0.58$ m/s) to point d ($u = 85$ m/s or $U = 0.85$ m/s), the pressure drop continues to decrease with the increasing u but with a different trend from that between points b and c. Point c is one of the important turning points on the pressure drop curve in the flow ascending process. When the gas velocity exceeds 85 m/s, the pressure drop rises slightly with the increasing u before it meets an obvious decrease at the point e. The regime from points c to e is labeled as local mixing in Figure 2.

At point e ($u = 88$ m/s, $U = 0.88$ m/s), the internal spout suddenly breaks through the layer of Cylinder A particles and throws some glass beads on the bed surface. This state is quite unstable with a quite small fountain intermittently appearing and disappearing, and correspondingly the pressure drop still jumps between 3.1 kPa (point f) and 3.4 kPa (point e). It should be noted that, the term of "a small fountain"

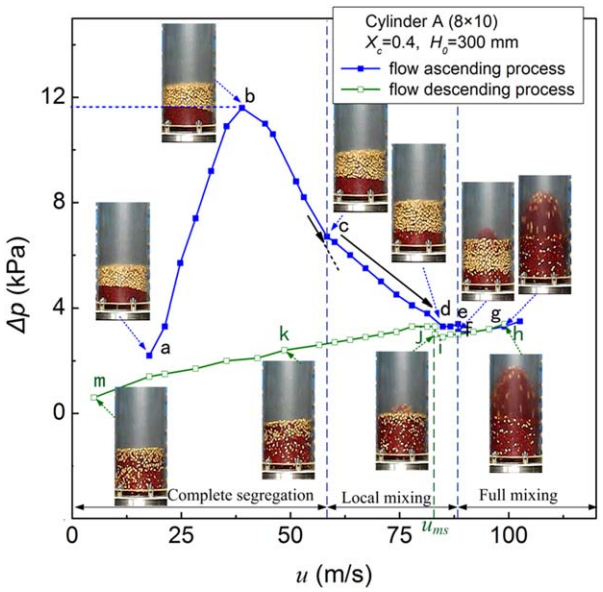

Figure 2. Evolutions of flow patterns and total pressure drops in gas flow ascending and descending processes with Cylinder A and glass beads ($H_0 = 300$ mm, $X_c = 0.4$).

[Color figure can be viewed in the online issue, which is available at wileyonlinelibrary.com.]

not only refers to that the height of fountain is very low but also the scope covered by the fountain is very narrow in the bed surface. Only the cylindroid particles within the central region of the column are involved into the spouting, while the cylindroid particles near the wall only slightly vibrate at their respective positions or even remain stagnant. The poor flowability and larger size of cylindroid particles make them difficult to entrain for a small fountain, which means that the first cycle in the spouted bed is very local. This small fountain holds for only several seconds and then collapses. When the fountain disappears, all the visible bamboo particles are stagnant or only slight vibrate, and a degree of segregation is obviously observed between the bamboo particles and glass beads which have mixed together during the previous cycle. After several seconds, the internal jet rebreaks through the bed surface and forms an external fountain. This state that fountain intermittently appears and disappears reflects the hysteresis effect of the current system.

Once the gas flow rate exceeds 88 m/s (i.e, the superficial gas velocity exceeds 0.88 m/s), a continuous and obviously higher fountain quickly forms and all particles in beds start to move. The cylindroid particles and glass beads are perfectly mixed and circularly move together in the bed. After stable external spouting forms, the increase in gas velocity still brings out a slowly rising pressure drop, as shown as the regime labeled as full mixing in Figure 2. This phenomenon is somewhat different from that in the spouted bed handling a single kind of fine spherical particles, in which the pressure drop is usually reported as a roughly constant value with further increase in gas velocity.

In the total flow ascending process, the regime of local mixing is the peculiar stage for spouting the binary system which is initially layered. At point c, the internal spout just reaches the interface between glass beads and cylindroid particles, while it has extended through the layer of bamboo particles and near to the upper bed surface at point d. The

difference in properties and compaction states of particles under and above the interface is believed to be responsible for the change in pressure drop trends before and after point c. The pressure drop in the flow ascending process is ascribed to the weight and compaction of the curvature region right above the roof of the internal spout.[9] Before the point c, the internal jet is within the layer of glass bead. With the increasing gas flow rate, the jet gradually expands, resulting in the gradual decrease of the glass beads above the roof of the inter spout. This decrease of glass beads with large density leads to the rapidly decreasing pressure drop in Figure 2. However, after point c, it is the lighter bamboo particles above the roof of internal jet that gradually decrease with the increasing gas flow rate, which results in the obviously less rapid decrease in pressure drop. For the small growth in pressure drop from points d and e, the possible reason is that when the top of spout is approaching the upper bed surface, the fine glass beads are thrown upward into the space between the bamboo particles, which decreases the void fraction between particles and increases the mass above the roof of the internal spout, resulting in the slight increase in the pressure drop.

The similar distribution of pressure drop vs. superficial gas velocity was reported in a spouted bed equipped with nonporous draft tube by Altzibar et al.[15,16] On pressure drop curve of the bed with nonporous draft tube, there is also a special turning point during the pressure drop decreases from the maximum value to the value of fountain formation with the increasing air velocity. Before and after this point, the pressure drop trends are different. Unfortunately, the authors[15,16] did not provide the detailed information on the turning point. However, it is worth noting that both in the spouted bed with nonporous draft tube and in the current one handling the two kinds of particles that are initially layered, the spouts will go through two different regions. In the spouted bed with nonporous draft tube, the two regions are entrainment zone and tube zone, while in the current bed the spout will go through the layer of glass beads and the layer of bamboo particles. Zhao et al.[17] proposed a promising approach to calculate the pressure drop of fixed beds in which only a part of the cross section of the bed is passed by the injected gas. They introduced a factor k for the superficial gas velocity to account for the uneven gas distribution in the cross section of their tapered fluidized bed without a gas distributor, as shown in Eq. 1

$$\Delta P_{\mathrm{f}} = \mathrm{C_1H_0}\frac{D_0}{D_1}U^* + \mathrm{C_2H_0}\frac{D_0(D_0^2+D_0D_1+D_1^2)}{3{D_1}^2}U^* + \frac{1}{2}\left(\frac{U^*}{\varepsilon_0}\right)^2\left[\left(\frac{D_0}{D_1}\right)^2-1\right]\rho \tag{1}$$

where $U^* = kU = 3.5U$, $C_1 = (150(1-\varepsilon_0)^2/\varepsilon_0^3)(\mu/(\varphi d_{\mathrm{p}})^2)$ and $C_2 = (1.75(1-\varepsilon_0)/\varepsilon_0^3)(\rho/(\varphi d_{\mathrm{p}}))$.

In this study, for the binary system of Cylinder A particles and glass beads with $H_0 = 300$ mm, $X_{\mathrm{c}} = 0.4$, and $U = 0.389$ m/s, the calculated peak pressure drop based on Eq. 1 is $\Delta p_{\mathrm{max,cal}} = 1.9$ kPa, while the experimental result is $\Delta p_{\mathrm{max,exp}} = 11.6$ Kpa. The significant deviation between the calculated and experimental results mainly relies on several reasons. Equation 1 was derived from a tapered fluidized bed,[17] while here it is used in a spouted bed. The gas–solid flow in a cylindrical-conical spouted bed is quite different from that in a tapered fluidized bed, even though they are both in apparently fixed state. Additionally, the current system contains two kinds of initially segregated particles, which makes the definition of parameters in Eq. 1 somewhat doubtful. It should be pointed that Eq. 1 is still a quite promising prediction for pressure drop in fluidized beds but necessary validation or modification is required when it is applied in spouted beds.

The spouting behaviors of binary mixture with Cylinder A particles and glass beads in the gas flow descending process also have been investigated in this work and the detailed information is revealed in Figure 2. When gas velocity decreases from 95 to 86 m/s, one can observe that the fountain in the bed becomes shorter, and the rate of particle circulation is slower. Particles in annulus consequently move down very slowly. A few of bamboo particles even stagnate on edge of the bed surface. Slight local segregation can be first observed on the bed surface. During this process, the total pressure drop decreases slowly, following the similar patch to that in the ascending process, until it suddenly elevates at $u = 84$ m/s ($U = 0.84$ m/s). With $u = 84$ m/s ($U = 0.84$ m/s), stable external spouting disappears. Only a very small fountain intermittently occurs with the pressure drop correspondingly jumping between points i and j. Obvious local segregation also happens in the annulus, which will become more significant when the fountain collapses. External spouting can be maintained at a considerably lower gas velocity in the gas flow descending process. In this study, the inlet gas velocity corresponding to points i and j is defined as the inlet-based minimum spouting velocity, u_{ms}. The superficial minimum spouting velocity is $U_{\mathrm{ms}} = u_{\mathrm{ms}}/100$.

With the further decreasing gas flow rate, the fountain disappears completely, and more bamboo particles are elevated to the upper bed level, resulting in the increasingly obvious local segregation. The total pressure drop decreases, following a quite different path, with a much lower pressure drop than for the ascending process. When the inlet gas velocity decreases to approximately zero, the cylindroid bamboo particles tend to distribute in the upper part of the bed. From the bed surface to the bottom, the concentration of bamboo particles declines, while the glass beads show the completely different distribution. There is no clear interface between these two kinds of particles.

In conclusion, in the spouted bed handling the binary system of cylindroid bamboo particles and glass beads with the proper particle properties and volume ratio, once the gas velocity exceeds the minimum spouting velocity and the resulting stable external spouting takes place, the cylindroid particles and glass beads will fully mix with each other and stably circulate together through the spout region, fountain region, and annulus region. During the stable spouting, that is, the normal operating status in a spouted bed reactor, segregation phenomenon never happens. The segregation only appears when gas velocity is lower than the minimum spouting velocity, which is an apparently improper operating condition. The proper volume ratio and the minimum spouting velocity are the key parameters that directly determine both the stable spouting and full mixing. This is quite different from the observation in the fluidized beds which is characterized with the complicated and indistinct relationships between the fluidization regimes and the mixing and segregation phenomena.[5,18,19] The minimum spouting velocity in a spouted bed has been found to depend on various factors, such as the reactor configuration, the prosperities of particles

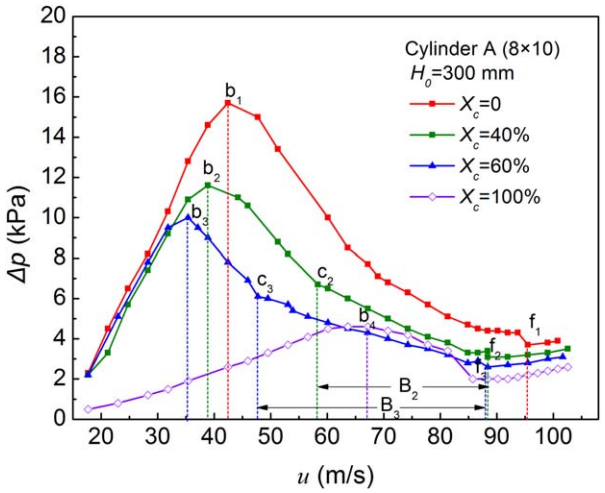

Figure 3. Evolutions of total pressure drop in the gas flow ascending when handling Cylinder A and glass beads with varying X_c (H_0 = 300 mm).

[Color figure can be viewed in the online issue, which is available at wileyonlinelibrary.com.]

and gas, and the operating conditions.[9] However, this study is focused on the treatment on the binary system of cylinders and spheres in a spouted bed, and therefore, the proper volumetric ratio and the effect of volume ratio on the minimum spouting velocity will be emphatically discussed in the following sections.

Characteristics of pressure drops

Effects of Volume Fraction of Cylindroid Particles on the Pressure Drop. The volume fraction of cylindroid particles, X_c, in the spouted bed, reflecting the biomass ratio that the unit handles in practical applications, is one of the important design parameters. The volume fraction of Cylinder A particles is varied from 0 to 1.0 in this study to investigate the effects of X_c on the total pressure drop in the bed, while the total static bed height is kept as $H_0 = 300$ mm. Typical curves of pressure drop in the flow ascending process are illustrated in Figure 3.

In Figure 3, the increase in X_c leads to the decreasing total pressure drop in their ascending processes. The pressure drop in the flow ascending process is ascribed to the weight and compaction of the curvature region right above the roof of the internal spout,[9] and properties of particles above the roof of the internal spout significantly affect the pressure drop. When X_c increases, the amount of bamboo particles with lower density increases, while the amount of glass beads with higher density decreases, which effectively reduces the weight of particles above the roof of the internal spout. When stable spouting forms in the bed with perfect mixing taking place, the increase in X_c effectively reduces the bulk density in the column, which needs lower pressure drop to support the spouting.

Figure 3 also shows the obvious difference in the distribution trends of pressure drops with different X_c. For the binary systems with $X_c = 0.4$ and 0.6, in which bamboo particles and glass beads initially layered in the bed, the regime of local mixing of $X_c = 0.6$ (labeled as B_3) is obviously wider than that of $X_c = 0.4$ (B_2). Δp_{max} always comes out in the regimes of complete segregation, and the bed with lager X_c encounters its smaller maximum pressure drop at the lower gas velocity. When X_c increases from 0.4 to 0.6, the layer of glass beads becomes thinner, causing that the turning point c_3 comes at the lower gas velocity than c_2 dose.

Above phenomenon, however, never happens when spouting pure glass beads ($X_c = 0$) or pure bamboo particles ($X_c = 1.0$). Compared with aforementioned evolutions of pressure drop, there are many other unique and interesting phenomena in spouting the pure nonspherical bamboo particles with larger size and lower density ($X_c = 1.0$ in Figure 3), which will be discuss in detail in our another work.

Effects of Particle Size on the Pressure Drop. In the thermochemical conversion of biomass, the size and shape of biomass particles is another important factor to affect the operational efficiency of the spouted beds. Therefore, three kinds of bamboo particles, that is, Cylinder A ($d \times l = 8 \times 10$ mm^2), Cylinder B (4×10 mm^2), and Cylinder C (4×20 mm^2), are adopted to preliminarily investigate the effects of particle size and shape on the flow behaviors in the bed under the condition that $X_c = 0.4$ and $H_0 = 300$ mm. Detailed properties of these three kinds of particles are shown in Table 1.

The pressure drop distributions of three kinds of bamboo particles, respectively, mixing with glass beads are illustrated in Figure 4. Three curves are in similar trends, and three regimes, as well as the key points, defined in Figure 2 can be explicitly distinguished in each curve.

However, the differences in diameter and height of cylinders cause their differences in packing void fraction, equivolume sphere diameter, aspect ratio (or sphericity), and these complicated features combined with the special structure of the bed, lead to obvious differences in the three pressure drop curves. The curve corresponding to Cylinder C with the largest aspect ratio is the first to encounter its peak value (point b_3), followed by the curve of Cylinder B and the curve of Cylinder A, while the values of Δp_{max} are successively larger. The curve of Cylinder C also encounters its turning point c_3 at a lowest gas velocity, while the curve of Cylinder A encounters its turning point c_1 at the highest gas velocity.

The maximum pressure drops of these binary systems take place before their internal spout beds extend into the layer of bamboo particles, and therefore, the shape and size of

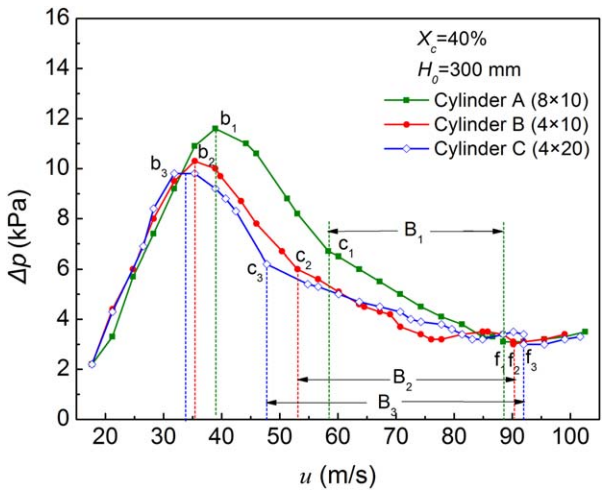

Figure 4. Evolutions of total pressure drop in the gas flow ascending when handling glass beads and different cylindroid particles (H_0 = 300 mm, X_c = 0.4).

[Color figure can be viewed in the online issue, which is available at wileyonlinelibrary.com.]

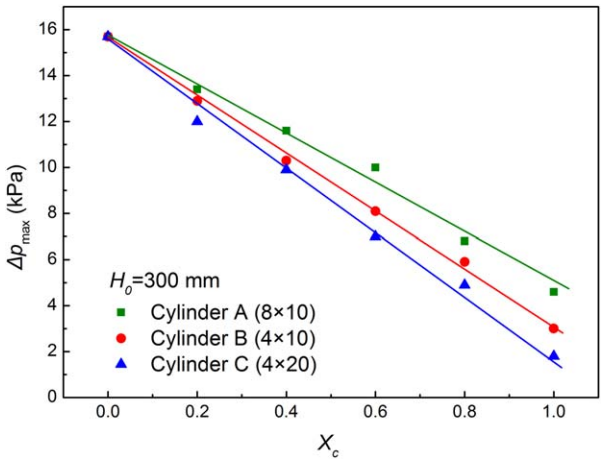

Figure 5. The maximum pressure drop when handling glass beads and different cylindroid particles with varying X_c ($H_0 = 300$ mm).

[Color figure can be viewed in the online issue, which is available at wileyonlinelibrary.com.]

bamboo particles are not able to directly affect the evolution of the internal spouts. But the Cylinder A particles have a lowest packing void fraction, which means, with the same packing volume, this kind of particles will have the greatest mass compared to the other kinds of cylinders. The greatest mass right above the roof of internal spout most seriously suppresses the development of the internal spout and the system needs highest gas velocity to reach its largest Δp_{max} and to expand through the layer of glass beads. For the Cylinder C with high aspect ratio, its highest packing void fraction leads to the fastest growing internal spout in the bed, and therefore, the corresponding curves reaches its Δp_{max} at the lowest gas velocity. The packing void fraction is considered as the main factor to affect the evolution of pressure drop in the layer of glass beads.

When the internal spouts extends into the layer of bamboo particles, the shape and size of bamboo particles, determining their flowability, will directly influence the flow behaviors in beds, which results in the complicated pressure drop distributions in regimes of local mixing. Cylinder A particles have the highest sphericity, and thus, the best flowability, which leads to that curve of Cylinder A in Regime B_1 is smooth and the pressure drop decreases near linearly with the increasing gas velocity, while the lower sphericities of Cylinders B and C (or the higher aspect ratio), causing the worse flowability, make their curves in Regime B_2 and Regime B_3 more fluctuant. In addition, the worse flowability is bad for the development of internal spout, and thus, the curve of Cylinder C goes through the widest Regime B_3, finally, obtaining the stable spouting (point f_3) at the highest gas velocity, while the curve of Cylinder A goes through the narrowest Regime B_1, obtaining its stable spouting (point f_1) at the lowest gas velocity. After the stable spouting forms, the pressure drops of three curves are very similar both in value and trend and the possible reason is that when stable spouting takes place, the bamboo particles well mix with the glass beads and the flowability of this mixture mainly depends on the glass beads which is in majority in beds.

In addition, the maximum pressure drop, Δp_{max}, in the beds with varying volume fractions of Cylinder A, as well as Cylinders B and C, are illustrated in Figure 5. It reveals that X_c obviously influences Δp_{max}, and for the each kind of bamboo particles, Δp_{max} always near linearly decreases with the increasing X_c; for different cylindroid particles with the same X_c, the particles with larger packing void fraction will be of the lower Δp_{max}.

Δp_{max} is recommended to be proportion to the bulk density of bed, ρ_b, in the system of spouting homogenous particles.[20–22] However, for the binary systems with larger cylindroid particles and fine spherical particles which are initially layered, influences on Δp_{max} become more complicated. Here, with the increasing X_c, the decreasing mass in the region directly above the internal spout mainly contributes to the decrease of Δp_{max}. At the same static bed height, the increasing X_c, thickening the layer of bamboo particles in the initial bed, causes the linearly decrease in the mass above the internal spout, leading to the decreasing Δp_{max}. The larger packing void fraction in the layer of cylindroid particles will also reduce the mass above the internal spout, and then result in the decrease in Δp_{max}.

Minimum spouting velocity

The inlet-based minimum spouting velocity, u_{ms}, in binary systems is defined as the inlet gas velocity corresponding to the point (i.e., point i in the Figure 2) at which stable external spouting collapses in the flow descending process in this study. Figure 6 shows the detailed values of u_{ms} under different conditions. u_{ms} presents different change trends with the increasing X_c when handling the cylindroid particles with different equivolume diameter, d_v.

In the binary systems of glass beads and Cylinder A particles with the largest d_v, the minimum spouting velocity always increases with the increasing X_c. However, the increase in u_{ms} is quite slight when X_c is low, while when X_c is high, for example, $X_c = 0.6$, 0.8, and 1.0, the increase in u_{ms} with the growing X_c becomes very obvious.

For the Cylinders B with the smallest d_v, the minimum spouting velocity decreases slowly with X_c increasing from 0 to 0.8. However, when X_c continues to increase to 1.0, u_{ms} turns to increase. The sudden increase of u_{ms} is due to the

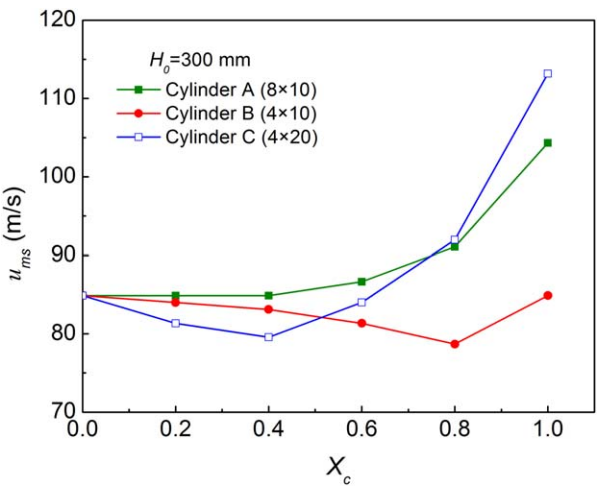

Figure 6. The inlet-based minimum spouting velocity when handling glass beads and different cylindroid particles with varying X_c ($H_0 = 300$ mm).

[Color figure can be viewed in the online issue, which is available at wileyonlinelibrary.com.]

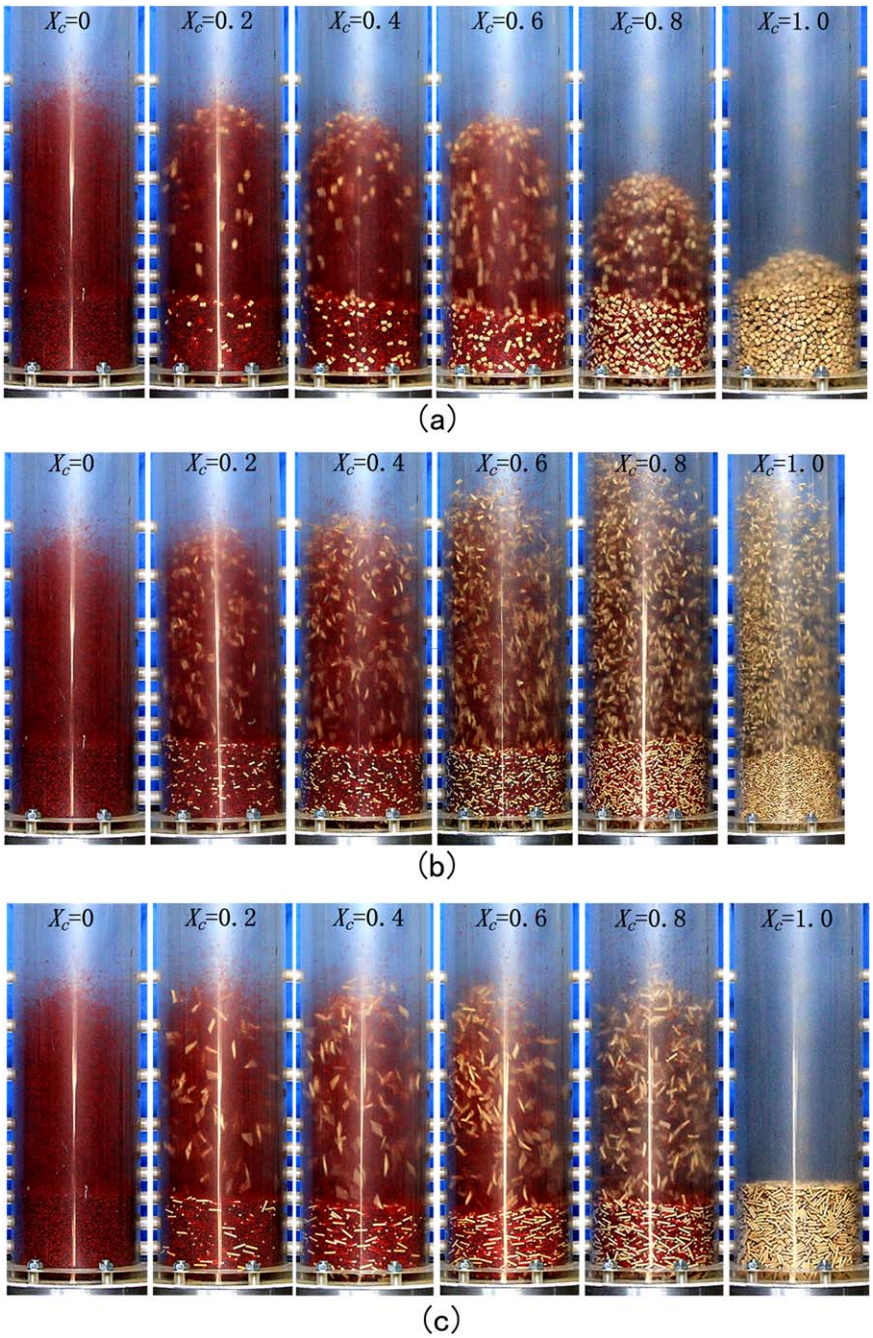

Figure 7. Snapshots of external spouting states handling the mixtures of glass beads and different cylindroid particles with varying X_c ($H_0 = 300$ mm, $u = 106$ m/s): (a) Cylinder A with $d_v = 9.9$ mm and $l/d = 1.25$; (b) Cylinder B with $d_v = 6.8$ mm and $l/d = 2.5$; (c) Cylinder C with $d_v = 7.2$ mm and $l/d = 5$.

[Color figure can be viewed in the online issue, which is available at wileyonlinelibrary.com.]

worse flowability of the pure bamboo particles which brings the significant hysteresis effects to the system.

In the binary system of Cylinders C with the medium d_v, the change of u_{ms} is more complicated. When X_c increases from 0 to 0.4, u_{ms} slowly decreases with the increasing X_c, while when X_c continues to increase from 0.4 to 0.8, u_{ms} turns to increase. When X_c is increased to 1.0, u_{ms} encounters a more dramatic increase.

In a spouted bed handling homogeneous spherical particles, u_{ms} is widely considered to be proportion to $d_p^m[(\rho_p - \rho)/\rho]^n$, in which d_p and ρ_p are the diameter and density of particles and ρ is the density of gas, and m, n are usually greater than 0.[9,13,23–27] For the binary mixture of cylindroid bamboo particles and glass beads, the increase in X_c leads to a increase in mean particle diameter and a decrease in bulk density of the bed, causing the change of u_{ms}. In the mixture of glass beads and Cylinder A particles, which have the large equivolume diameter, the increase in mean particle diameter caused by the increasing X_c overwhelms the decrease in bulk density of the bed, finally, resulting in the increasing u_{ms}. However, the situation of Cylinder B particles with the smallest equivolume diameter is just different, and the increase in mean particle diameter caused by the increasing X_c is just covered up by the decrease in bulk density of the bed, which results in the decreasing u_{ms}. In the mixture of glass beads and Cylinder C

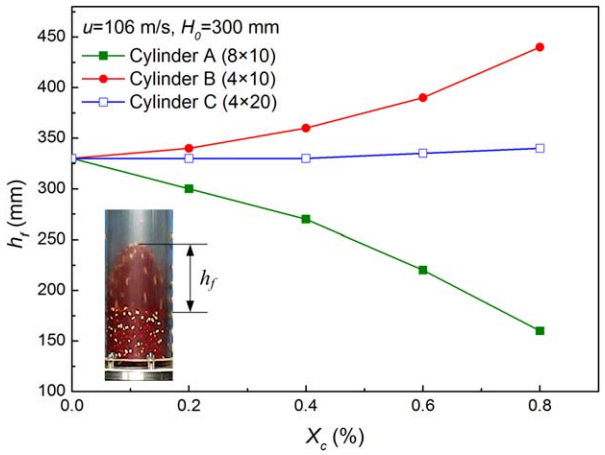

Figure 8. Fountain heights when spouting the mixtures of glass beads and different cylindroid particles with varying X_c (H_0 = 300 mm, u = 106 m/s).

[Color figure can be viewed in the online issue, which is available at wileyonlinelibrary.com.]

particles, aforesaid two situations alternately happen. In addition, due to the highest aspect ratio of Cylinder C, the worst flowability should be somewhat responsible for the dramatic increase in u_{ms} when X_c is large. When spouting the pure bamboo particles ($X_c = 1.0$), the low flowability of Cylinder B particles cause the u_{ms} turn to increase. The worst flowability of Cylinder C particles makes the bed need the highest u_{ms} to form external spouting.

Explanation above is only qualitative and more detailed information should be supplemented in the further work.

Characteristics of stable spouting

To more directly investigate and comprehend the spouting and mixing phenomenon in spouted beds, the snapshots of spouted beds with different particles and varying X_c are shown in Figure 7, and the corresponding fountain heights are illustrated in Figure 8. In all cases, the gas velocity is u = 106 m/s.

The maximum volume fraction of bamboo particles, $X_{c,max}$ in mixture

In Figure 7, when X_c of Cylinder A particles varies from 0 to 1.0, stable spouting can successfully forms in every case and in the cases of $X_c = 0.2$, 0.4, 0.6, and 0.8, the particles of Cylinder A mix very well with the glass beads. For Cylinder B particles, stable spouting and well mixing can take place under the conditions of $X_c \leq 0.6$ with the gas velocity of 106 m/s. When X_c is increased from 0.8 to 1.0, the fountain becomes unstable and leans toward the bed wall with increasingly high probability.

For Cylinder C particles, stable spouting and well mixing only can take place under the conditions of $X_c = 0$, 0.2, and 0.4. When $X_c = 0.6$, the fountain starts to lean toward the bed wall intermittently; when $X_c = 0.8$, the fountain always leans so that it is difficult to capture its height. When $X_c = 1.0$, external spouting even fails to form with the inlet gas velocity of 106 m/s in the flow ascending process. The high aspect ratio of Cylinder C particles results in their bad flowability, and mixing them with the fine spherical glass beads can effectively improve the flowability of the mixture. With increasing X_c, the volume fraction of glass beads decreases and the flowability of mixture in the bed become worse, which cause the fountain increasingly leaning. With continuously taking multiple shots, the instantaneously upright fountain was captured in the Figure 7.

For each kind of the bamboo particles, there is a maximum volume fraction of bamboo particles, $X_{c,max}$, to maintain the stable spouting with a certain gas velocity. $X_{c,max}$ is considered to be related to the flowability of bamboo particles, which depends on the aspect ratio of cylinders in this study. With the gas velocity of 106 m/s, $X_{c,max}$ of Cylinder A is 1.0, and for Cylinders B and C, $X_{c,max}$ is 0.6 and 0.4, respectively, which means that the cylindroid particles with larger aspect ratio will be of the less $X_{c,max}$ when they are mixed with the bed materials in spouted beds.

Fountain height

The fountain height, h_f, is defined as the distance from the surface of the annulus to the top of the fountain in this study, and the detailed values under different conditions are revealed in Figure 8.

These three kinds of particles show the entirely different changes of fountain height with varying X_c, as gas velocity is kept as 106 m/s, that is, $U = 1.06$ m/s. For Cylinder A particles, the fountain height decreases with the increasing X_c, while fountain height of Cylinder B obviously increases when X_c is increased. Different from both the situations of Cylinders A and B, the fountain height of Cylinder C only presents a quite slight increase with the increasing X_c. In addition, with the same X_c (expect for the cases of $X_c = 0$ and 1.0), the mixture including Cylinder B always achieves the highest fountain, while the mixtures including Cylinder A obtains the lowest fountain.

An obvious correspondence can be observed between the distributions of fountain height (in Figure 8) and the minim spouting velocity (in Figure 6) with X_c increasing from 0 to 0.8. When the gas velocity is equal to the minim spouting velocity, that is, $u/u_{ms} = 1$, the fountain height is immediately zero; the further increase in u/u_{ms} can generally lead to the increasing fountain height. For the binary system of Cylinder A particles and glass beads, the minimum spouting velocity, u_{ms}, has been found to increase with the increasing X_c. Thus, when u is kept as 106 m/s, u/u_{ms} will decrease with the increasing X_c, which consequently bring the decrease of fountain height. By the same token, for the binary system of Cylinder B particles and glass beads, with the increasing X_c (from 0 to 0.8), the decrease of u_{ms} leads to the increasing u/u_{ms}, which finally causes the increasing fountain height. However, the correspondence is less obvious for the binary system of Cylinder C particles and glass beads. This is somewhat due to the instable spoutings when $X_c > 0.4$, which cause corresponding fountain heights is less reliable.

Conclusions

The spouting and mixing behaviors of cylindroid particles and spherical particles in a spouted bed have been experimentally investigated. The characteristics of flow pattern and pressure drop of the binary mixture are figured out and three kinds of cylindroid particles with different sizes and shapes are involved in experiments to discuss the effects of particle size and shape on the spouting and mixing behaviors in beds. The emphasis is laid on the influence of the volume fraction of cylindroid particles on the spouting and mixing phenomena, including the total pressure drop, the minimum

spouting velocity and fountain height. For the binary systems with larger cylindroid and spherical particles which are initially layered in the bed, the following conclusions can be drawn from this work:

1. The transition of flow patterns and evolution of total pressure drop to spouted bed are generally similar to that of spouting homogenous spherical particles but accompanied by additional mixing and segregating behaviors. The earliest local mixing appears after the internal spout reaches the interface of two kinds of particles. When stable spouting forms, the cylindroid and spherical particles are mixed perfectly and cyclically move together. Once the fountain collapses, local segregation appears.
2. The evolution of total pressure drop in the flow ascending process can be divided into three regimes, that is, complete segregation, local mixing, and full mixing, based on the mixing states of cylindroid and spherical particles in the beds. At a certain static bed height, both the increase in the volume fraction of cylindroid particles, X_c, and the aspect ratio of cylindroid particles, l/d, will widen the regime of local mixing. The maximum total pressure drop, Δp_{max}, always appears in the regime of complete segregation, and it decreases with the increasing X_c or the increasing l/d of cylindroid particles.
3. The minimum spouting velocities, u_{ms}, of the binary mixture presents different change trends with the increasing X_c when handling the cylindroid particles with different equivolume diameter, d_v. With the increasing d_v, three possible situations in turn appear: u_{ms} may decreases, first decrease and then increase, or directly increase with the increasing X_c. The larger aspect ratio of cylinders also contributes to the increase of u_{ms}. Compared to spouting mixtures, a considerably larger u_{ms} is required to spouting the pure cylindroid particles.
4. After the external spouting forms, there is a maximum volume fraction, $X_{c,max}$, for each kind of cylindroid particles to maintain the stable fountain at a certain gas velocity. With the same gas velocity, $X_{c,max}$ is lower for the cylindroid particles with higher aspect ratio. With the same gas velocity and X_c, the mixture of spherical particles and cylinders with smaller d_v obtain the higher fountain height.

Acknowledgment

Financial supports from the National Natural Science Funds for Distinguished Young Scholar (No. 51325601), the Major Program of National Natural Science Foundation of China (No. 51390492), and the Jiangsu Natural Science Funds for Distinguished Young Scholar (No. BK20130022) are sincerely acknowledged.

Notation

Asr = aspect ratio, dimensionless
D = diameter of the column, m
D_0 = diameter of bed where air nozzles located, m
D_1 = diameter of the upper base of the initial particle bed, m
D_i = diameter of gas inlet, m
d = diameter of cylinder, mm
d_p = diameter of particles, mm
d_v = equivolume diameter, mm
H_0 = static bed height, mm
h_f = fountain height, mm
Δp = total pressure drop, kPa
Δp_f = pressure drop in fixed bed, Pa
Δp_{max} = the maximum pressure drop, kPa
l = length of cylinder, mm
U = superficial gas velocity, m/s
U^* = modified superficial gas velocity, m/s
u = inlet-based gas velocity, m/s
U_{ms} = superficial minimum spouting velocity, m/s
u_{ms} = inlet-based minimum spouting velocity, m/s
μ = gas viscosity, Pa s
V = volume of particles, m^3
V_c = volume of cylindroid particles, m^3
X_c = volume fraction of cylindroid particles, dimensionless
$X_{c,max}$ = the maximum volume fraction of cylindroid particles, dimensionless
ε_0 = packing void fraction, dimensionless
ρ = gas density, kg/m^3
ρ_p = particles density, kg/m^3
ρ_b = the bulk density of bed, kg/m^3
φ = particle sphericity, dimensionless

Literature Cited

1. Cui HP, Grace JR. Fluidization of biomass particles: a review of experimental multiphase flow aspects. *Chem Eng Sci*. 2007;62(1–2):45–55.
2. Bridgwater AV. Renewable fuels and chemicals by thermal processing of biomass. *Chem Eng J*. 2003;91(2–3):87–102.
3. Mohan D, Pittman CU, Steele PH. Pyrolysis of wood/biomass for bio-oil: a critical review. *Energy Fuels*. 2006;20(3):848–889.
4. Bridgwater AV, Peacocke GVC. Fast pyrolysis processes for biomass. *Renew Sustain Energy Rev*. 2000;4(1):1–73.
5. Zhang Y, Jin BS, Zhong WQ. Experimental investigation on mixing and segregation behavior of biomass particle in fluidized bed. *Chem Eng Process Process Intensification*. 2009;48(3):745–754.
6. Bridgwater AV. Review of fast pyrolysis of biomass and product upgrading. *Biomass Bioenergy*. 2012;38:68–94.
7. Ren B, Zhong WQ, Jin BS, Shao YJ, Yuan ZL. Numerical simulation on the mixing behavior of corn-shaped particles in a spouted bed. *Powder Technol*. 2013;234:58–66.
8. Lathouwers D, Bellan J. Modeling of dense gas-solid reactive mixtures applied to biomass pyrolysis in a fluidized bed. *Int J Multiphase Flow*. 2001;27(12):2155–2187.
9. Epstein N, Grace JR. *Spouted and Spout-Fluid Beds: Fundamentals and Applications*. England: Cambridge University Press, 2011.
10. Olazar M, San Jose MJ, Penas FJ, Aguayo AT, Bilbao J. Stability and hydrodynamics of conical spouted beds with binary mixtures. *Ind Eng Chem Res*. 1993;32(11):2826–2834.
11. Olazar M, San Jose MJ, Lamosas RL, Bilbao J. Hydrodynamics of sawdust and mixtures of wood residues in conical spouted beds. *Ind Eng Chem Res*. 1994;33(4):993–1000.
12. Zhong WQ, Jin BS, Zhang Y, Wang XF, Xiao R. Fluidization of biomass particles in a gas-solid fluidized bed. *Energy Fuels*. 2008;22(6):4170–4176.
13. Shao YJ, Zhong WQ, Chen X, Chen Y, Jin BS. Spouting of non-spherical particles in conical-cylindrical spouted bed. *Can J Chem Eng*. 2014;92(4):742–746.
14. Devahastin S, Mujumdar AS. Some hydrodynamic and mixing characteristics of a pulsed spouted bed dryer. *Powder Technol*. 2001;117:189–197.
15. Altzibar H, Lopez G, Bilbao J, Olazar M. Operating and peak pressure drops in conical spouted beds equipped with draft tubes of different configuration. *Ind Eng Chem Res*. 2014;53:415–427.
16. Altzibar H, Lopez G, Bilbao J, Olazar M. Minimum spouting velocity of conical spouted beds provided with draft tubes of different configuration. *Ind Eng Chem Res*. 2013;52:2995–3006.
17. Zhao ZG, Zhang JW, Zhang GY, Zeng X, Liu XX, Xu GW. Hydrodynamic characterization of a tapered gas-solid bed without a gas distributor. *Powder Technol*. 2014;256:300–309.
18. Olivieri G, Marzocchlla A, Salatino P. A fluid-bed continuous classifier of polydisperse granular solids. *J Taiwan Inst Chem Eng*. 2009;40:638–644.
19. Marzocchella A, Salatino P, Di Pastena V, Lirer L. Transient fluidization and segregation of binary mixtures of particles. *AIChE J*. 2000;46(11):2175–2182.
20. Asenjo JA, Muñoz R, Pyle DL. On the transition from a fixed to a spouted bed. *Chem Eng Sci*. 1977;32(2):109–117.
21. Kmieć A. Hydrodynamics of flows and heat transfer in spouted beds. *Chem Eng J*. 1980;19(3):189–200.

22. Rocha SCS, Taranto OP, Ayub GE. Aerodynamics and heat transfer during coating of tablets in two-dimensional spouted bed. *Can J Chem Eng*. 1995;73(3):308–312.
23. Mathur KB, Gishler PE. A technique for contacting gases with coarse solid particles. *AIChE J*. 1955;1:157–164.
24. Fane AG, Mitchell RA. Minimum spouting velocity of scaled-up beds. *Can J Chem Eng*. 1984;62:437–439.
25. Choi M, Meisen A. Hydrodynamics of shallow, conical spouted beds. *Can J Chem Eng*. 1992;70:916–924.
26. Olazar M, San José MJ, Aguayo AT, Arandes JM, Bilbao J. Hydrodynamics of nearly flat base spouted beds. *Chem Eng J Biochem Eng J*. 1994;55(1–2):27–37.
27. Zhong WQ, Liu XJ, Grace JR, Epstein N, Ren B, Jin BS. Prediction of minimum spouting velocity of spouted bed by CFD-TFM: scale-up. *Can J Chem Eng*. 2013;91(11):1809–1814.

Manuscript received Mar. 31, 2014, and revision received July 16, 2014.